Islet, Majuro Atoll

Chapter 7
Marshall Islands

Introduction

This chapter provides a brief description of the Marshall Islands, its past and present climate as well as projections for the future. The climate observation network and the availability of atmospheric and oceanic data records are outlined. The annual mean climate, seasonal cycles and the influences of large-scale climate features such as the Intertropical Convergence Zone and patterns of climate variability (e.g. the El Niño-Southern Oscillation) are analysed and discussed. Observed trends and analysis of air temperature, rainfall, extreme events, sea-surface temperature, ocean acidification, mean and extreme sea levels are presented. Projections for air and sea-surface temperature, rainfall, sea level, ocean acidification and extreme events for the 21st century are provided. These projections are presented along with confidence levels based on expert judgement by Pacific Climate Change Science Program (PCCSP) scientists. The chapter concludes with summary tables of projections for the northern and southern Marshall Islands (Tables 7.4 and 7.5). Important background information including an explanation of methods and models is provided in Chapter 1. For definitions of other terms refer to the Glossary.

7.1 Climate Summary

7.1.1 Current Climate

- Air temperatures show very little seasonal variation, with the mean maximum temperatures in the warmest months less than 2ºF (1ºC) warmer than those in the coldest months.

- The Marshall Islands experiences a wet season from May to November and a dry season from December to April, but rainfall varies greatly from north to south.

- The Intertropical Convergence Zone brings rainfall to the Marshall Islands throughout the year. It is strongest and furthest north and closest to the Marshall Islands during the wet season, and it is weakest and furthest away from the islands to the south in the dry season.

- The main influence on year-to-year natural climate variability in the Marshall Islands is the El Niño-Southern Oscillation.

- Warming trends are evident in both annual and seasonal mean air temperatures at Majuro for the period 1956–2009 and at Kwajalein for the period 1960–2009.

- The Majuro (1954–2009) and Kwajalein (1950–2009) negative annual and dry season rainfall trends are statistically significant. Wet season rainfall trends over the respective periods for both sites are not significant.

- The sea-level rise, measured by satellite altimeters since 1993, is about 0.3 inches (7 mm) per year.

- Droughts and storm waves are the main extreme events that impact the Marshall Islands. Tropical cyclones (typhoons) usually form between September and November but are often weak when they pass through the Marshall Islands' region.

7.1.2 Future Climate

Over the course of the 21st century:

- Surface air temperature and sea-surface temperature are projected to continue to increase (*very high* confidence).

- Annual and seasonal mean rainfall is projected to increase (*high* confidence).

- The intensity and frequency of days of extreme heat are projected to increase (*very high* confidence).

- The intensity and frequency of days of extreme rainfall are projected to increase (*high* confidence).

- The incidence of drought is projected to decrease (*moderate* confidence).

- Tropical cyclone numbers are projected to decline in the tropical North Pacific Ocean basin (0–15ºN, 130ºE –180ºE) (*moderate* confidence).

- Ocean acidification is projected to continue (*very high* confidence).

- Mean sea-level rise is projected to continue (*very high* confidence).

7.2 Country Description

Located near the equator in the central North Pacific Ocean, the Marshall Islands lie between 4°N–14°N and 160°E–173°E. The country consists of 29 low-lying atolls and five low-elevation islands, with a total land area of 70 square miles (181 km²). This is in contrast to the 700 000 square miles of ocean (1.81 million km²) which forms the country's Exclusive Economic Zone.

The atolls and islands lie in two parallel chains: Ratak (Sunrise) to the east; and Ralik (Sunset), to the west (Marshall Islands' First National Communication under the UNFCCC, 2000; Marshall Islands' Pacific Adaptation to Climate Change, 2010). The capital is Majuro in the Ratak island chain. The 2010 estimated population was 54 439 (Marshall Islands Country Statistics, SOPAC, 2010).

Key economic sectors are services, agriculture and fisheries, and industry. The main industries are copra, tuna processing, tourism and handicrafts (Office of Environmental Policy Coordination, 2005).
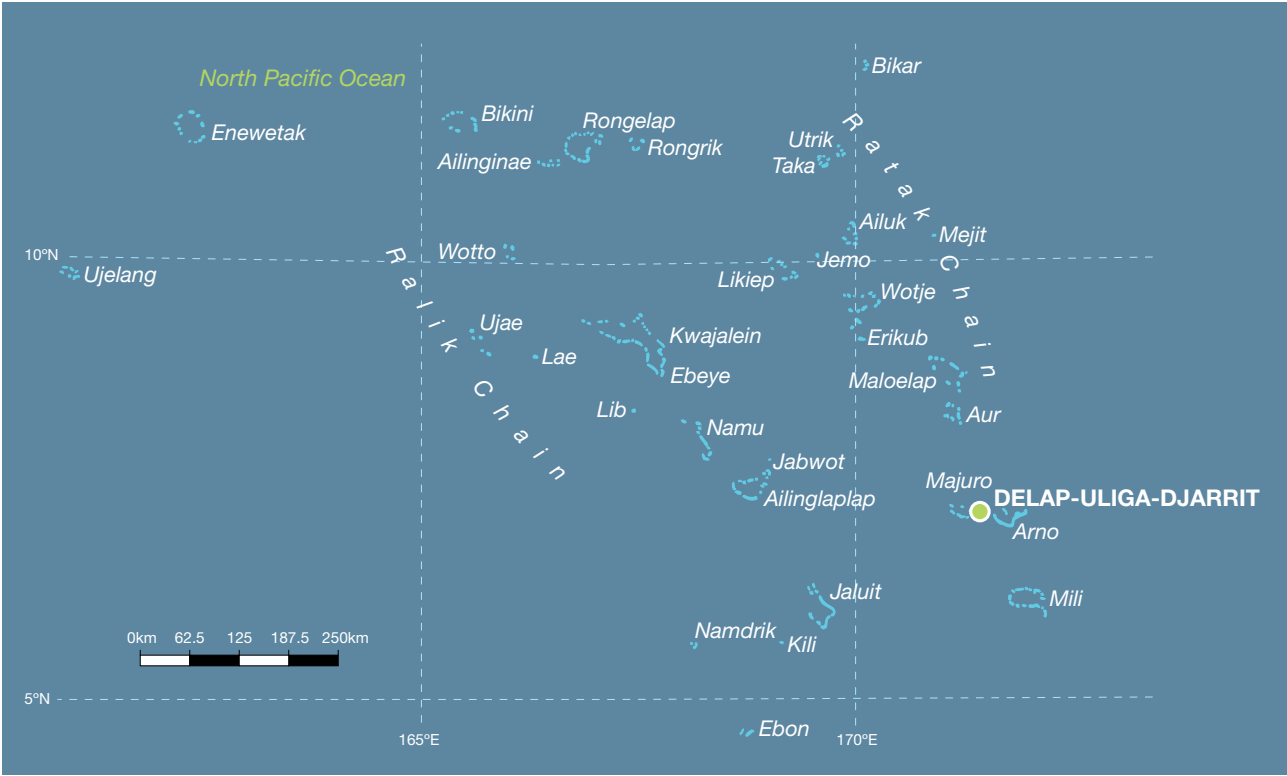

Figure 7.1: Marshall Islands

7.3 Data Availability

There are currently ten operational meteorological stations in the Marshall Islands. Multiple observations within a 24-hour period are taken at eight of these stations (Majuro, Utirik, Ailinglaplap, Jaluit, Wotje, Mili, Amata Kabua International Airport and Kwajalein) and a single daily observation is taken at Laura and Arno. The primary stations are located at Majuro (the capital) on the southern end of the Ratak chain and at Kwajalein near the centre of the Ralik chain (Figure 7.1). Observations began at Majuro in 1951 and at Kwajalein in 1949.

Records from 1951 for rainfall and from 1956 for temperature at Majuro have been used, as well as records from 1950 for rainfall and from 1960 for air temperature at Kwajalein. Both records are homogeneous and more than 99% complete.

There are a number of sea-level records available for the Marshall Islands. The best appear to be Enewetok (1951–1972), Kwajalein (1946–present), Majuro-B (1968–2001) and Majuro-C (1993–2009). A global positioning system instrument to estimate vertical land motion was deployed in the Marshall Islands in 2007 and will provide valuable direct estimates of local vertical land motion in future years. Both satellite (from 1993) and in situ sea-level data (1950–2009; termed reconstructed sea level; Volume 1, Section 2.2.2.2) are available on a global 1° x 1° grid.

Long-term locally-monitored sea-surface temperature data are unavailable for the Marshall Islands, so large-scale gridded sea-surface temperature datasets have been used (HadISST, HadSST2, ERSST and Kaplan Extended SST V2; Volume 1, Table 2.3).

Weather balloon launch, Marshall Islands National Weather Service

7.4 Seasonal Cycles

Temperatures at both Majuro and Kwajalein are constant year-round because the amount of solar radiation does not vary significantly throughout the year (Figure 7.2). The mean maximum air temperatures in the warmest months are less than 2°F (1°C) warmer than those in the coldest months. The sea-surface temperature surrounding the small islands influences the seasonal cycles in air temperature.

The rainfall of the Marshall Islands varies greatly from north to south. The atolls at 10ºN and further north receive less than 50 inches (1250 mm) of rain annually and are very dry in the dry season. Atolls 7ºN and equatorward receive more than 100 inches (2500 mm) of rain annually. Both Majuro and Kwajalein have a dry season from around December to April and a wet season from May to November. The difference between the seasons is more marked at Kwajalein where the driest months (January–March) receive about 4 inches (100 mm) on average and the wettest months (September–October) receive on average around 12 inches (300 mm).

The Intertropical Convergence Zone (ITCZ) brings rainfall to the Marshall Islands throughout the year. The ITCZ is strongest and furthest north, and therefore closest to the Marshall Islands, during the wet season, and it is weakest and furthest away from the islands to the south in the dry season. The West Pacific Monsoon (WPM) affects the Marshall Islands in some years. Rainfall during a given year can be influenced by trade wind troughs, the Madden Julian-Oscillation (Volume 1, Section 2.4.4), the tropical upper tropospheric trough and the North Pacific sub-tropical high.

Mean Annual Climate Cycle
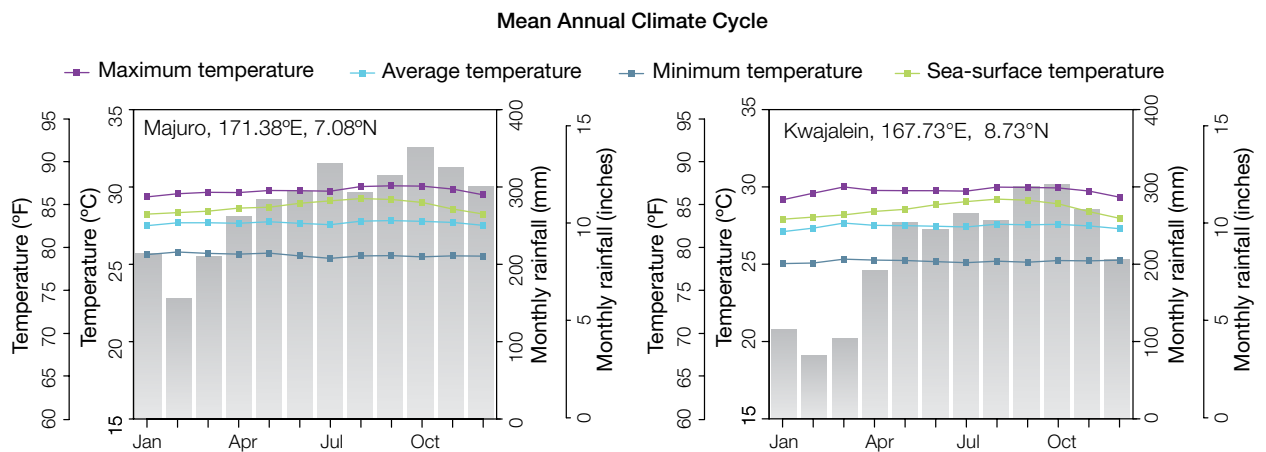
Figure 7.2: Mean annual cycle of rainfall (grey bars) and daily maximum, minimum and mean air temperatures at Majuro (left) and Kwajalein (right), and local sea-surface temperatures derived from the HadISST dataset (Volume 1, Table 2.3).

7.5 Climate Variability

The main influence on the year-to-year natural climate variability in the Marshall Islands is the El Niño-Southern Oscillation (ENSO), as seen in the correlation coefficients between climate indices and rainfall and air temperatures at Majuro (Table 7.1) and Kwajalein (Table 7.2). Rainfall variability is high at both sites, with the wettest years bringing up to twice as much rain as the driest years. The influence of ENSO in producing this variability can be clearly seen (Figure 7.4) with La Niña events being significantly wetter than El Niño years. At both sites wet season maximum and minimum air temperatures are influenced by ENSO. El Niño events tend to bring above average wet season air temperatures. During the dry season the influence of El Niño is to bring warmer than average minimum air temperatures as well as below average rainfall. The reason for these changes is that El Niño results in the ITCZ moving to the south of the Marshall Islands which leads to lower rainfall when El Niño is firmly established. There is also the competing influence of the WPM in the wet season which is able to reach the Marshall Islands in El Niño years when easterly trade winds are weak. ENSO Modoki events (Volume 1, Section 3.4.1) have similar influences but only on temperature.

Table 7.1: Correlation coefficients between indices of key large-scale patterns of climate variability and minimum and maximum temperatures (Tmin and Tmax) and rainfall at Majuro. Only correlations statistically different from zero (95% level) are shown.

Climate feature/index		Wet season (May-October)			Dry season (November-April)		
		Tmin	Tmax	Rain	Tmin	Tmax	Rain
ENSO	Niño3.4	0.31	0.59		0.41		-0.49
	Southern Oscillation Index	-0.27	-0.51		-0.30		0.48
Interdecadal Pacific Oscillation Index							
ENSO Modoki Index			0.44		0.37		
Number of years of data		54	54	56	54	54	56

Table 7.2: Correlation coefficients between indices of key large-scale patterns of climate variability and minimum and maximum temperatures (Tmin and Tmax) and rainfall at Kwajalein. Only correlations statistically different from zero (95% level) are shown.

Climate feature/index		Wet season (May-October)			Dry season (November-April)		
		Tmin	Tmax	Rain	Tmin	Tmax	Rain
ENSO	Niño3.4	0.36	0.48			0.37	-0.37
	Southern Oscillation Index	-0.32	-0.47			-0.35	0.33
Interdecadal Pacific Oscillation Index							
ENSO Modoki Index			0.53			0.46	
Number of years of data		50	50	65	49	49	65

7.6 Observed Trends

7.6.1 Air Temperature

Warming trends of a similar magnitude are evident in both annual and seasonal mean air temperatures at Majuro (1956–2009) and Kwajalein (1960–2009). Annual and seasonal minimum air temperature trends are stronger than those for maximum air temperatures at Majuro (Figure 7.3 and Table 7.3).

7.6.2 Rainfall

The Majuro (1954–2009) and Kwajalein (1950–2009) negative annual and dry season rainfall trends are statistically significant. Wet season rainfall trends over the respective periods for both sites are not significant (Table 7.3 and Figure 7.4).

7.6.3 Extreme Events

Droughts and storm waves are the main extreme events that impact the Marshall Islands. Droughts generally occur in the first four to six months of the year following an El Niño. During severe El Niño events, rainfall can be suppressed by as much as 80%. The dry season begins earlier and ends much later than normal. ENSO events also modulate sea level, and this modulation can significantly hamper ground water extraction.


Annual Mean Temperature – Majuro

Annual Mean Temperature – Kwajalein
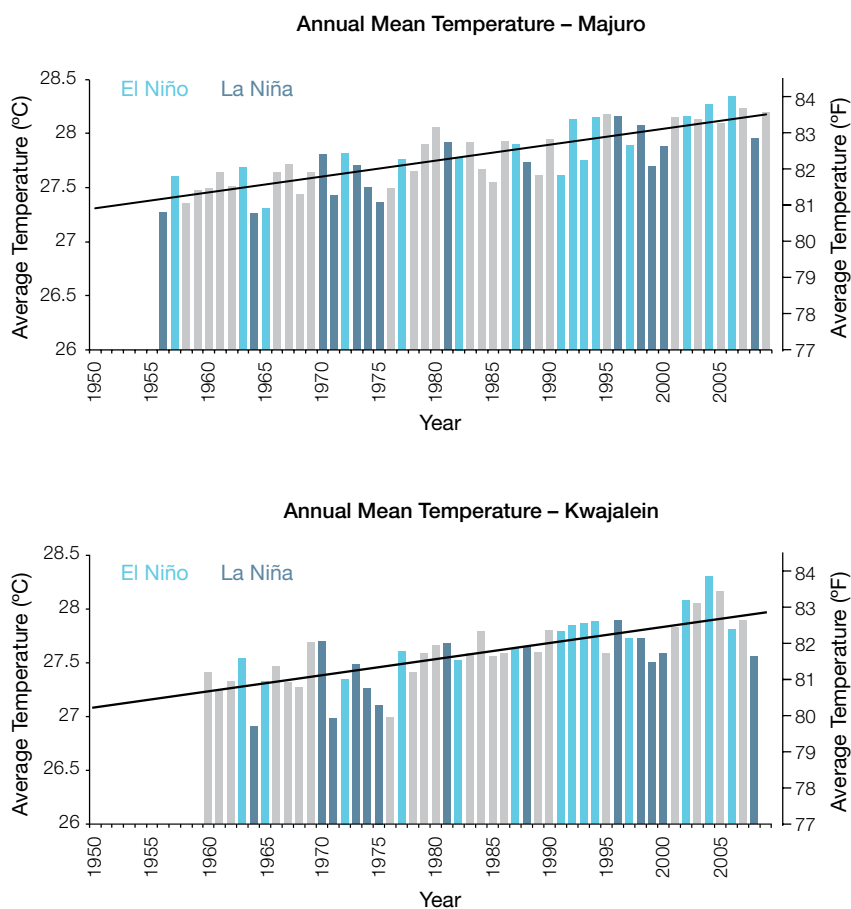
Figure 7.3: Annual mean air temperature at Majuro (top) and Kwajalein (bottom). Light blue, dark blue and grey bars denote El Niño, La Niña and neutral years respectively.

Table 7.3: Annual and seasonal trends in maximum, minimum and mean air temperature (Tmax, Tmin and Tmean) and rainfall at Majuro and Kwajalein for the period 1950–2009[a]. Asterisks indicate significance at the 95% level. Persistence is taken into account in the assessment of significance as in Power and Kociuba (in press). The statistical significance of the air temperature trends is not assessed.

	Majuro Tmax °F per 10 yrs (°C per 10 yrs)	Majuro Tmin °F per 10 yrs (°C per 10 yrs)	Majuro Tmean °F per 10 yrs (°C per 10 yrs)	Majuro Rain inches per 10 yrs (mm per 10 yrs)	Kwajalein Tmax °F per 10 yrs (°C per 10 yrs)	Kwajalein Tmin °F per 10 yrs (°C per 10 yrs)	Kwajalein Tmean °F per 10 yrs (°C per 10 yrs)	Kwajalein Rain inches per 10 yrs (mm per 10 yrs)
Annual	+0.21 (+0.12)	+0.31 (+0.17)	+0.26 (+0.15)	-4.18* (-106)	+0.29 (+0.16)	+0.25 (+0.14)	+0.27 (+0.15)	-3.31* (-84)
Wet season	+0.20 (+0.11)	+0.35 (+0.20)	+0.28 (+0.16)	-2.79 (-71)	+0.33 (+0.18)	+0.25 (+0.14)	+0.29 (+0.16)	-1.86 (-47)
Dry season	+0.23 (+0.13)	+0.27 (+0.15)	+0.25 (+0.14)	-1.48* (-38)	+0.24 (+0.13)	+0.26 (+0.14)	+0.25 (+0.14)	-1.47* (-37)

[a] Majuro rainfall from 1954 and air temperature from 1956, Kwajalein air temperature from 1960.

Annual Rainfall – Majuro


Annual Rainfall – Kwajalein
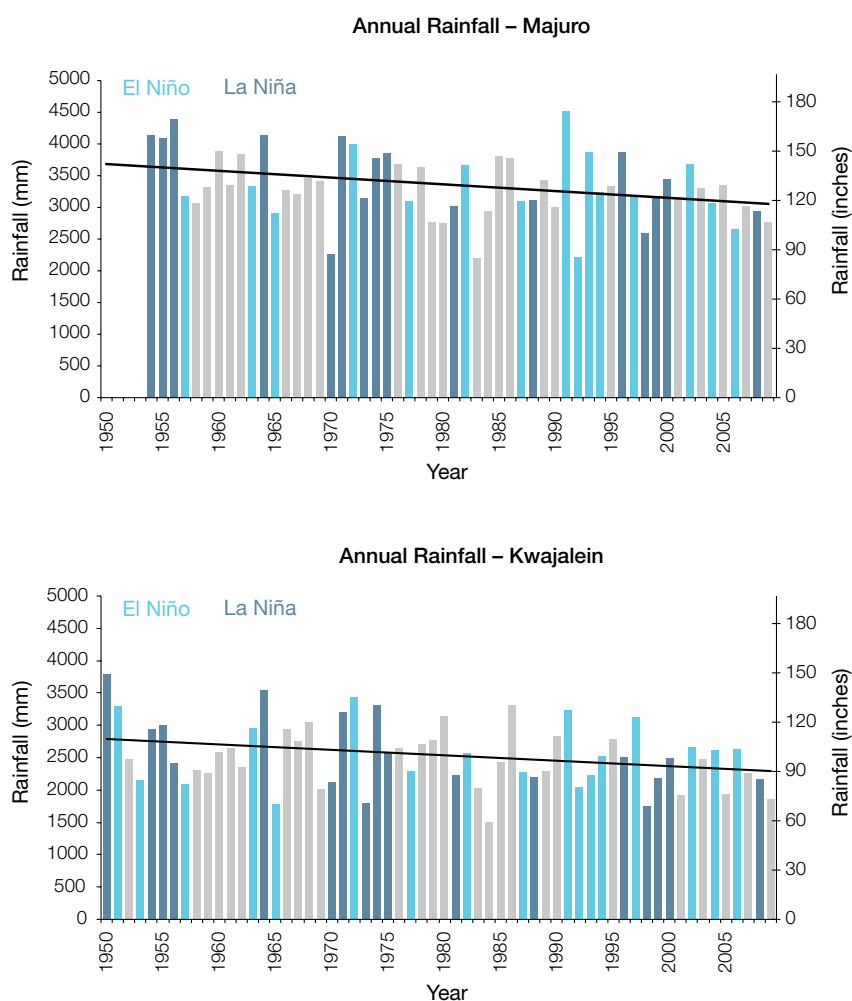
Figure 7.4: Annual rainfall at Majuro (top) and Kwajalein (bottom). Light blue, dark blue and grey bars denote El Niño, La Niña and neutral years respectively.

In December 2008 the islands were impacted several times in quick succession by long-period swell waves generated by an extra-tropical storm. These extreme waves, combined with high tides, caused widespread flooding in Majuro and other urban centres, which are located about a metre above sea level. A state of emergency was declared on Christmas morning.

Tropical cyclones usually form between September and November and are often weak when they pass through the region. During El Niño years, however, sea-surface temperatures increase to the east of the Marshall Islands. This favours more intense tropical cyclones in the Marshall Islands region.

7.6.4 Sea-Surface Temperature

Historical changes in sea-surface temperature around the Marshall Islands show considerable decadal variability. Figure 7.7 shows the 1950–2000 sea-surface temperature changes (relative to a reference year of 1990) from three different large-scale sea-surface temperature gridded datasets (HadSST2, ERSST and Kaplan Extended SST V2; Volume 1, Table 2.3). Water temperatures remained relatively constant from the 1950s to the late 1980s around the southern islands, while they declined slightly around the northern islands.

Since the 1970 both regions have shown warming trends (approximately 0.07°C per decade in the north and approximately 0.09°C per decade in the south). At these regional scales, natural variability may play a large role in the sea-surface temperature trends making it difficult to identify any long-term trends.

7.6.5 Ocean Acidification

Based the large-scale distribution of coral reefs across the Pacific and the seawater chemistry, Guinotte et al. (2003) suggested that seawater aragonite saturation states above 4 were optimal for coral growth and for the development of healthy reef ecosystems, with values from 3.5 to 4 adequate for coral growth, and values between 3 and 3.5, marginal. Coral reef ecosystems were not found at seawater aragonite saturation states below 3 and these conditions were classified as extremely marginal for supporting coral growth.

In the Marshall Islands region, the aragonite saturation state has declined from about 4.5 in the late 18th century to an observed value of about 3.9 ± 0.1 by 2000.

7.6.6 Sea Level

Monthly averages of the historical tide gauge, satellite (since 1993) and gridded sea-level (since 1950) data agree well after 1993 and indicate interannual variability in sea levels of about 20 cm (estimated 5–95% range) after removal of the seasonal cycle (Figure 7.9). The sea-level rise near the Marshall Islands measured by satellite altimeters (Figure 7.5) since 1993 is about 0.3 inches (7 mm) per year, more than the global average of 0.125 ± 0.015 inches (3.2 ± 0.4 mm) per year. This rise is partly linked to a pattern related to climate variability from year to year and decade to decade (Figure 7.9).

Regional Distribution of the Rate of Sea-Level Rise
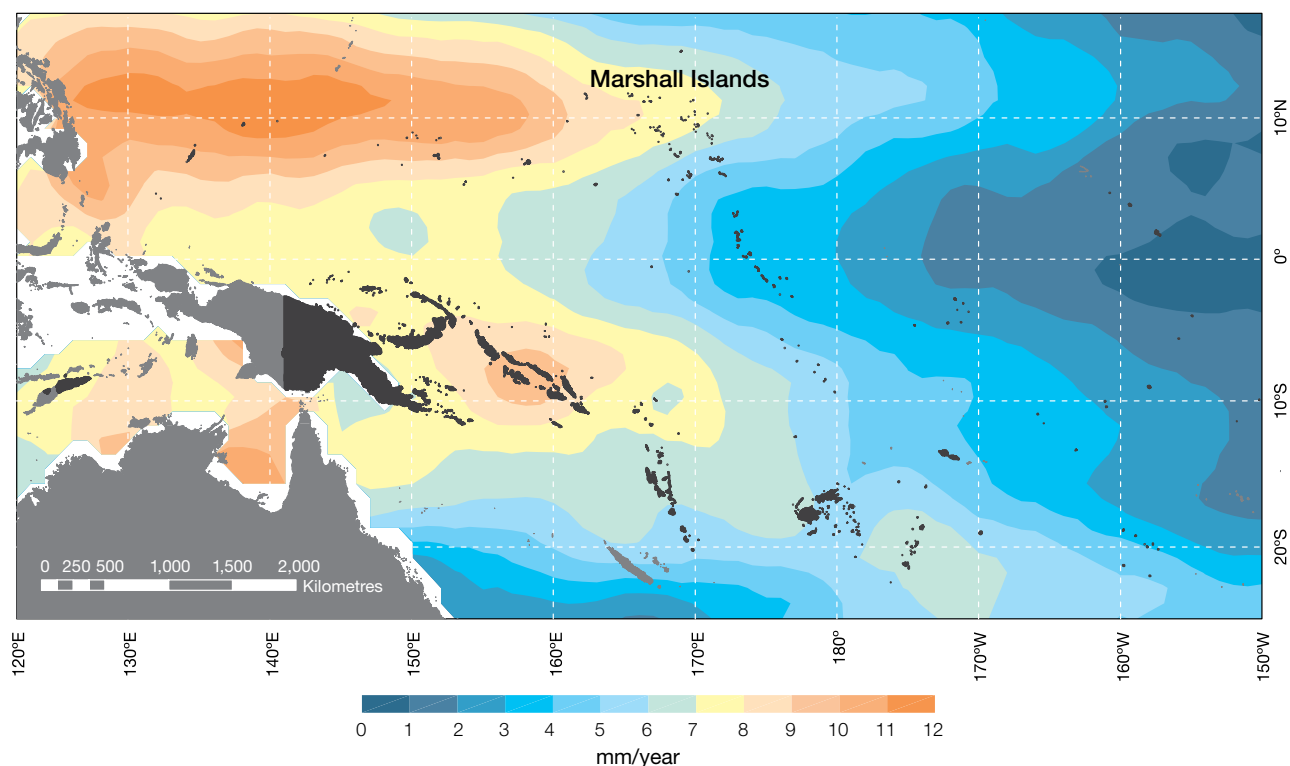
Figure 7.5: The regional distribution of the rate of sea-level rise measured by satellite altimeters from January 1993 to December 2010, with the location of the Marshall Islands indicated. Further information on regional distribution of sea-level rise is provided in Volume 1, Section 3.6.3.2.

7.6.7 Extreme Sea-Level Events

The annual climatology of the highest daily sea levels has been evaluated from hourly measurements by tide gauges at Majuro and Kwajalein (Figure 7.6). Highest tides at both locations tend to occur around the equinoxes, with lower high tides tending to occur towards the solstices.

This interannual (spring) tidal height variability is more pronounced at Majuro than at Kwajalein. Seasonal and short-term components show relatively little variation throughout the year at both locations. Sea levels are usually lower in El Niños and higher in La Niñas. The top 10 recorded water levels at both locations cluster around the equinoxial tidal peaks, especially at Majuro. Of these, six occur during

La Niña conditions and only one during El Niño conditions at Majuro. At Kwajalein, three of the top 10 water levels occur during La Niña and none during El Niño. At both locations, the relatively strong annual variability in tidal heights recorded by the tide gauges indicates this is a significant component of observed high water level events.
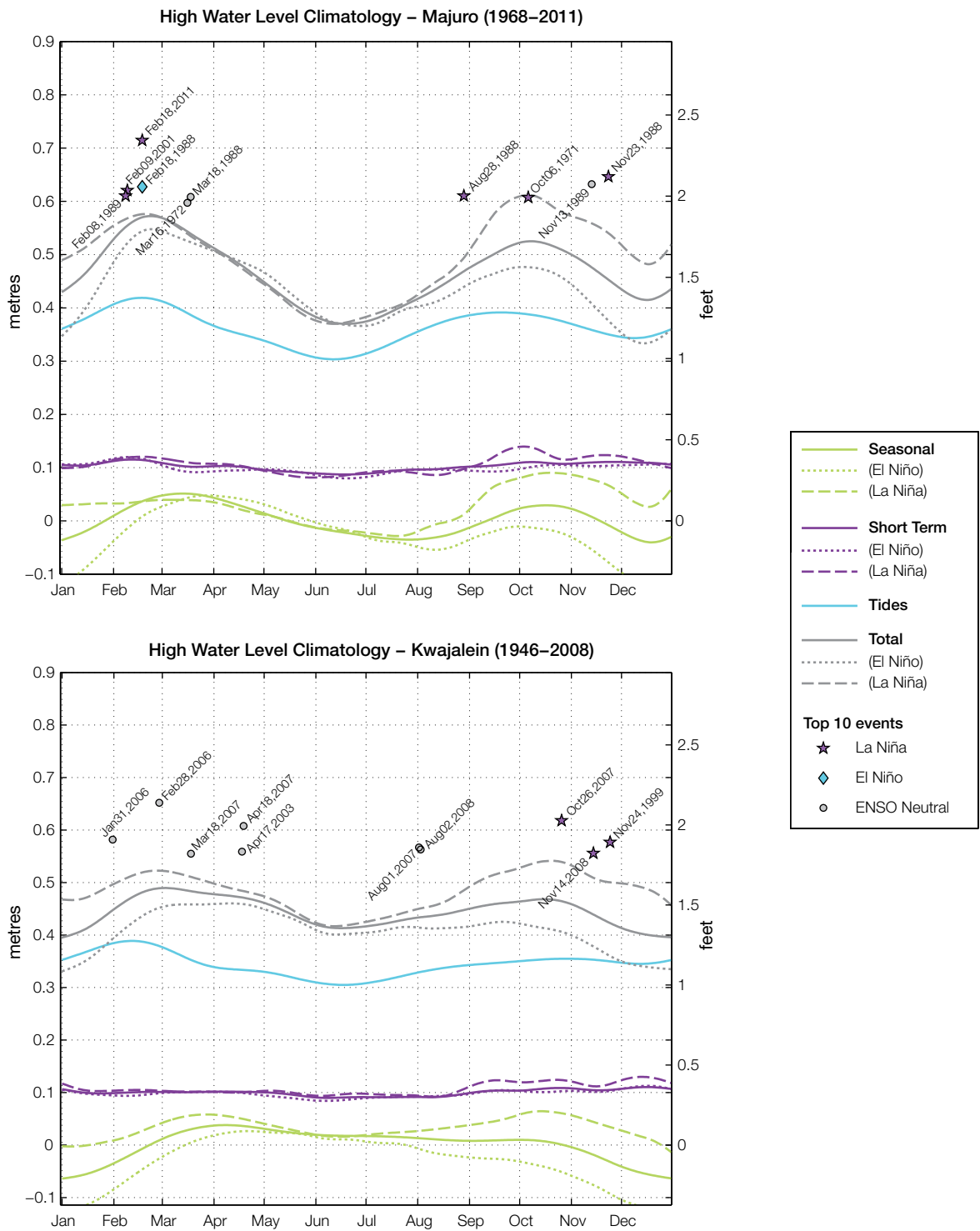
Figure 7.6: The annual cycle of high water relative to Mean Higher High Water (MHHW) due to tides, short-term fluctuations (most likely associated with storms) and seasonal variations for Majuro (top) and Kwajalein (bottom). The tides and short-term fluctuations are respectively the 95% exceedence levels of the astronomical high tides relative to MHHW and short-term sea-level fluctuations. Components computed only for El Niño and La Niña years are shown by dotted and dashed lines, and grey lines are the sum of the tide, short-term and seasonal components. The 10 highest sea-level events in the record relative to MHHW are shown and coded to indicate the phase of ENSO at the time of the extreme event.

7.7 Climate Projections

Climate projections have been derived from up to 18 global climate models from the CMIP3 database, for up to three emissions scenarios (B1 (low), A1B (medium) and A2 (high)) and three 20-year periods (centred on 2030, 2055 and 2090, relative to 1990). These models were selected based on their ability to reproduce important features of the current climate (Volume 1, Section 5.2.3), so projections from each of the models are plausible representations of the future climate. This means there is not one single projected future for the Marshall Islands, but rather a range of possible futures. The full range of these futures is discussed in the following sections.

These projections do not represent a value specific to any actual location, such as a town or city in the Marshall Islands. Instead, they refer to an average change over the broad geographic region encompassing the Marshall Islands and the surrounding ocean. Projections refer to the entire Marshall Islands unless otherwise stated. In some instances, given that there are some differences between the climate of the northern and southern Marshall Islands (Section 7.4), projections are given separately for these two regions (Figure 1.1 shows the regional boundaries). Section 1.7 provides important information about interpreting climate model projections.

7.7.1 Temperature

Surface air temperature and sea-surface temperature are projected to continue to increase over the course of the 21st century. There is *very high* confidence in this direction of change because:

- Warming is physically consistent with rising greenhouse gas concentrations.
- All CMIP3 models agree on this direction of change.

The majority of CMIP3 models simulate a slight increase (<1.8°F; <1°C) in annual and seasonal mean temperature by 2030, however by

2090 under the A2 (high) emissions scenario temperature increases of greater than 4.5°F (2.5°C) are simulated by almost all models (Tables 7.4 and 7.5). Given the close relationship between surface air temperature and sea-surface temperature, a similar (or slightly weaker) rate of warming is projected for the surface ocean (Figure 7.7). There is *moderate* confidence in this range and distribution of possible futures because:

- There is generally a large discrepancy between modelled and observed temperature trends over the past 50 years in the vicinity

of the Marshall Islands, although this may be partly due to limited observational records (Figure 7.7).

Interannual variability in surface air temperature and sea-surface temperature over the Marshall Islands is strongly influenced by ENSO in the current climate (Section 7.5). As there is no consistency in projections of future ENSO activity (Volume 1, Section 6.4.1), it is not possible to determine whether interannual variability in temperature will change in the future. However, ENSO is expected to continue to be an important source of variability for the Marshall Islands and the region.
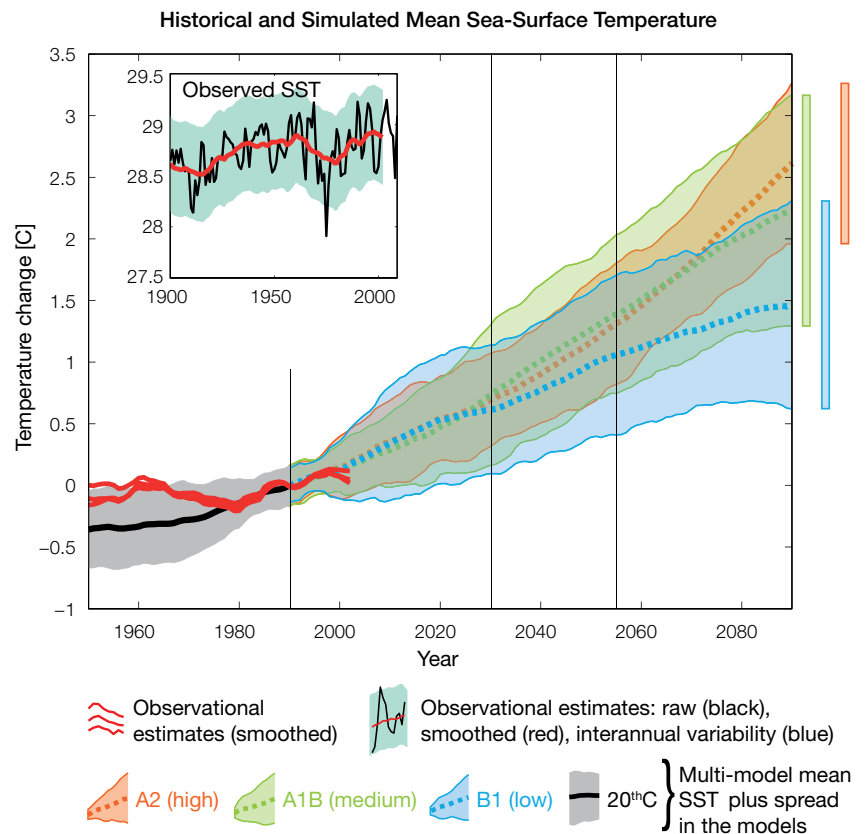
Figure 7.7: Historical climate (from 1950 onwards) and simulated historical and future climate for annual mean sea-surface temperature (SST) in the region surrounding the southern Marshall Islands, for the CMIP3 models. Shading represents approximately 95% of the range of model projections (twice the inter-model standard deviation), while the solid lines represent the smoothed (20-year running average) multi-model mean temperature. Projections are calculated relative to the 1980–1999 period (which is why there is a decline in the inter-model standard deviation around 1990). Observational estimates in the main figure (red lines) are derived from the HadSST2, ERSST and Kaplan Extended SST V2 datasets (Volume 1, Section 2.2.2). Annual average (black) and 20-year running average (red) HadSST2 data is also shown inset. Projections for the northern Marshall Islands closely resemble those for the south and are therefore not shown.

7.7.2 Rainfall

Wet season (May-October), dry season (November-April) and annual average rainfall is projected to increase over the course of the 21st century. There is *high* confidence in this direction of change because:

- Physical arguments indicate that rainfall will increase in the equatorial Pacific in a warmer climate (IPCC, 2007; Volume 1, Section 6.4.3).
- Almost all of the CMIP3 models agree on this direction of change by 2090.

The majority of CMIP3 models simulate little change (-5% to 5%) in rainfall by 2030, however by 2090 the majority simulate an increase (>5%) in wet season, dry season and annual rainfall. In fact, approximately one third of models simulate a large increase (>15%) in rainfall under the higher (i.e. A1B (medium) and A2 (high)) emissions scenarios, for the dry season in the northern Marshall Islands and on both a seasonal and annual basis in the south (Tables 7.4 and 7.5). There is *moderate* confidence in this range and distribution of possible futures because:

- In simulations of the current climate, the CMIP3 models broadly capture the influence of the ITCZ on the rainfall of the Marshall Islands (Volume 1, Sections 5.2.3.4 and 5.2.3.5).
- The CMIP3 models are unable to resolve many of the physical processes involved in producing rainfall. As a consequence, they do not simulate rainfall as well other variables, such as temperature (Volume 1, Chapter 5).

The inconsistency between the projected increase in annual and seasonal rainfall and the recent declining trends observed for Majuro and Kwajalein (Section 7.6.2) may be related to local factors not captured by the models (e.g. topography), or the fact that the projections presented here represent an average over a very large geographic region (Sections 1.7.1 and 1.7.2).

Interannual variability in rainfall over the Marshall Islands is strongly influenced by ENSO in the current climate (Section 7.5). As there is no consistency in projections of future ENSO activity (Volume 1, Section 6.4.1), it is not possible to determine whether interannual variability in rainfall will change in the future.

7.7.3 Extremes

Temperature

The intensity and frequency of days of extreme heat are projected to increase over the course of the 21st century. There is *very high* confidence in this direction of change because:

- An increase in the intensity and frequency of days of extreme heat is physically consistent with rising greenhouse gas concentrations.
- All CMIP3 models agree on the direction of change for both intensity and frequency.

For both the northern and southern Marshall Islands, the majority of CMIP3 models simulate an increase of approximately 2°F (1°C) in the temperature experienced on the 1-in-20-year hot day by 2055 under the B1 (low) emissions scenario, with an increase of over 4.5°F (2.5°C) simulated by the majority of models by 2090 under the A2 (high) emissions scenario (Tables 7.4 and 7.5). There is *low* confidence in this range and distribution of possible futures because:

- In simulations of the current climate, the CMIP3 models tend to underestimate the intensity and frequency of days of extreme heat (Volume 1, Section 5.2.4).
- Smaller increases in the frequency of days of extreme heat are projected by the CCAM 60 km simulations.

Rainfall

The intensity and frequency of days of extreme rainfall are projected to increase over the course of the 21st century. There is *high* confidence in this direction of change because:

- An increase in the frequency and intensity of extreme rainfall is consistent with larger-scale projections, based on the physical argument that the atmosphere is able to hold more water vapour in a warmer climate (Allen and Ingram, 2002; IPCC, 2007). It is also consistent with physical arguments that rainfall will increase in the deep tropical Pacific in a warmer climate (IPCC, 2007; Volume 1, Section 6.4.3).
- Almost all of the CMIP3 models agree on this direction of change for both intensity and frequency.

For the northern and southern Marshall Islands, the majority of CMIP3 models simulate an increase of at least 0.8 inches (20 mm) in the amount of rain received on the 1-in-20-year wet day by 2055 under the B1 (low) emissions scenario, with an increase of at least 1.8 inches (45 mm) simulated by the majority of models by 2090 under the A2 (high) emissions scenario. The majority of models project that the current 1-in-20-year event will occur, on average, three to four times every year in the northern Marshall Islands by 2055 under the B1 (low) emissions scenario and four to five times every year in the southern Marshall Islands. By 2090, under the A2 (high) emissions scenario, the frequency increases to five to six times every year in the northern Marshall Islands and seven to eight times every year in the southern Marshall Islands. There is *low* confidence in this range and distribution of possible futures because:

- In simulations of the current climate, the CMIP3 models tend to underestimate the intensity and frequency of extreme rainfall (Volume 1, Section 5.2.4).

- The CMIP3 models are unable to resolve many of the physical processes involved in producing extreme rainfall.

Drought

The incidence of drought is projected to decrease over the course of the 21st century. There is *moderate* confidence in this direction of change because:

- A decrease in drought is consistent with projections of increased rainfall (Section 7.7.2).
- The majority of models agree on this direction of change for most drought categories.

For both the northern and southern Marshall Islands, the majority of CMIP3 models project that mild drought will occur approximately eight to nine times every 20 years in 2030 under all emissions scenarios, decreasing to six to seven times by 2090. The frequency of moderate drought over the northern Marshall Islands is projected to decrease from two to three times every 20 years under the A1B (medium) and A2 (high) emissions scenarios to once to twice by 2090, while under the B1 (low) emissions scenario the frequency of moderate drought remains approximately stable at once to twice every 20 years. Over the southern Marshall Islands, the frequency of moderate drought is projected to remain approximately stable at once to twice every 20 years under all emissions scenarios. The majority of CMIP3 models project that severe droughts will occur approximately once every 20 years across all time periods and emissions scenarios. There is *low* confidence in

this range and distribution of possible futures because:

- There is only moderate confidence in the range of rainfall projections (Section 7.7.2), which directly influences projections of future drought conditions.

Tropical Cyclones (typhoons)

Tropical cyclone numbers are projected to decline in the tropical North Pacific Ocean basin (0–15ºS, 130ºE–180ºE) over the course of the 21st century. There is *moderate* confidence in this direction of change because:

- Many studies suggest a decline in tropical cyclone frequency globally (Knutson et al., 2010).
- Tropical cyclone numbers decline in the tropical North Pacific Ocean basin in the majority of assessment techniques.

Based on the direct detection methodologies (Curvature Vorticity Parameter (CVP) and the CSIRO Direct Detection Scheme (CDD) described in Volume 1, Section 4.8.2), 80% of projections show no change or a decrease in tropical cyclone formation when applied to the CMIP3 climate models for which suitable output is available. When these techniques are applied to CCAM, 100% of projections show a decrease in tropical cyclone formation. In addition, the Genesis Potential Index (GPI) empirical technique suggests that conditions for tropical cyclone formation will become less favourable in the North Pacific Ocean basin, for the majority (70%) of analysed CMIP3 models. There is *moderate* confidence in this range and distribution of possible futures because in simulations of the current climate, the CVP, CDD and

GPI methods capture the frequency of tropical cyclone activity reasonably well (Volume 1, Section 5.4).

Consistent with this projected reduction in total cyclone numbers, five of the six 60 km CCAM simulations also show a decrease in the proportion of the most severe storms (those stronger than the current climate 90th percentile storm maximum wind speed). Most simulations project an increase in the proportion of storms occurring in the weaker categories. Associated with this is a reduction in cyclonic wind hazard.

7.7.4 Ocean Acidification

The acidification of the ocean will continue to increase over the course of the 21st century. There is *very high* confidence in this projection as the rate of ocean acidification is driven primarily by the increasing oceanic uptake of carbon dioxide, in response to rising atmospheric carbon dioxide concentrations.

Projections from all analysed CMIP3 models indicate that the annual maximum aragonite saturation state will reach values below 3.5 by about 2035 and continue to decline thereafter (Figure 7.8; Tables 7.4 and 7.5). There is *moderate* confidence in this range and distribution of possible futures because the projections are based on climate models without an explicit representation of the carbon cycle and with relatively low resolution and known regional biases.

The impact of acidification change on the health of reef ecosystems is likely to be compounded by other stressors including coral bleaching, storm damage and fishing pressure.

Maximum Annual Aragonite Saturation State – Southern Marshall Islands

Legend: A2 (high) mean — A1B (medium) mean — B1 (low) mean — — — Horizon
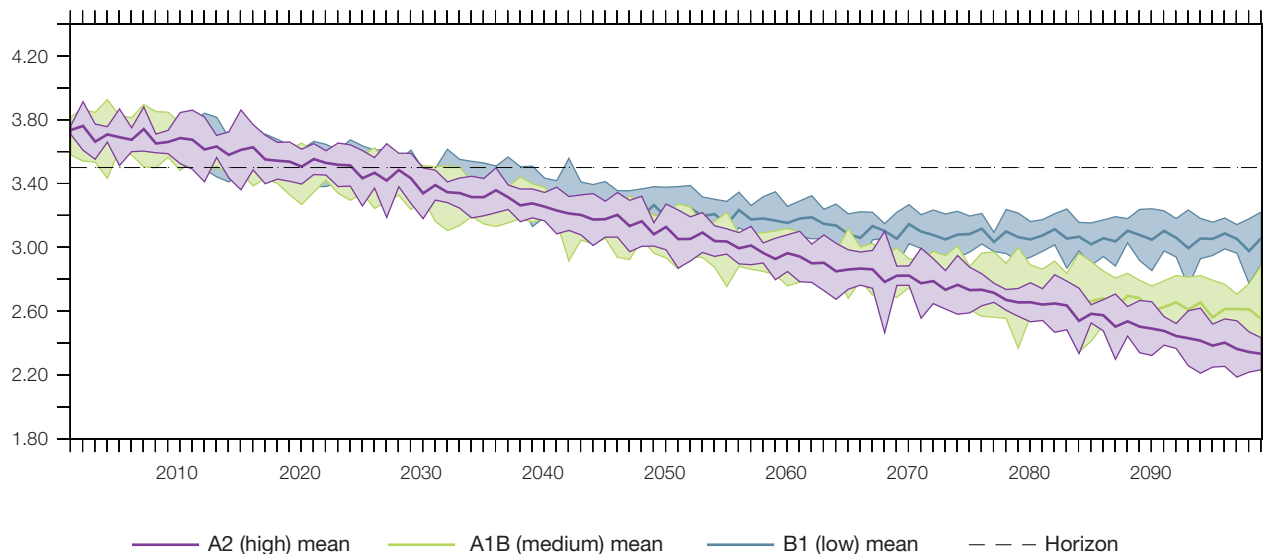
Figure 7.8: Multi-model projections, and their associated uncertainty (shaded area represents two standard deviations), of the maximum annual aragonite saturation state in the sea surface waters of the southern Marshall Islands under the different emissions scenarios. The dashed black line represents an aragonite saturation state of 3.5. Projections for the northern Marshall Islands closely resemble those for the south and are therefore not shown.

7.7.5 Sea Level

Mean sea level is projected to continue to rise over the course of the 21st century. There is *very high* confidence in this direction of change because:

- Sea-level rise is a physically consistent response to increasing ocean and atmospheric temperatures, due to thermal expansion of the water and the melting of glaciers and ice caps.
- Projections arising from all CMIP3 models agree on this direction of change.

The CMIP3 models simulate a rise of between approximately 2–6 inches (5–15 cm) by 2030, with increases of 8–24 inches (20–60 cm) indicated by 2090 under the higher emissions scenarios (i.e. A2 (high), A1B (medium); Figure 7.9; Tables 7.4 and 7.5).

There is *moderate* confidence in this range and distribution of possible futures because:

- There is significant uncertainty surrounding ice-sheet contributions to sea-level rise and a larger rise than that projected above cannot be excluded (Meehl et al., 2007b). However, understanding of the processes is currently too limited to provide a best estimate or an upper bound (IPCC, 2007).
- Globally, since the early 1990s, sea level has been rising near the upper end of the above projections. During the 21st century, some studies (using semi-empirical models) project faster rates of sea-level rise.

Interannual variability of sea level will lead to periods of lower and higher regional sea levels. In the past, this interannual variability has been about 8 inches (20 cm) (5–95% range, after removal of the seasonal cycle; dashed lines in Figure 7.9 (a)) and it is likely that a similar range will continue through the 21st century. In addition, winds and waves associated with weather phenomena will continue to lead to extreme sea-level events.

In addition to the regional variations in sea level associated with ocean and mass changes, there are ongoing changes in relative sea level associated with changes in surface loading over the last glacial cycle (glacial isostatic adjustment) and local tectonic motions. The glacial isostatic motions are relatively small for the PCCSP region.
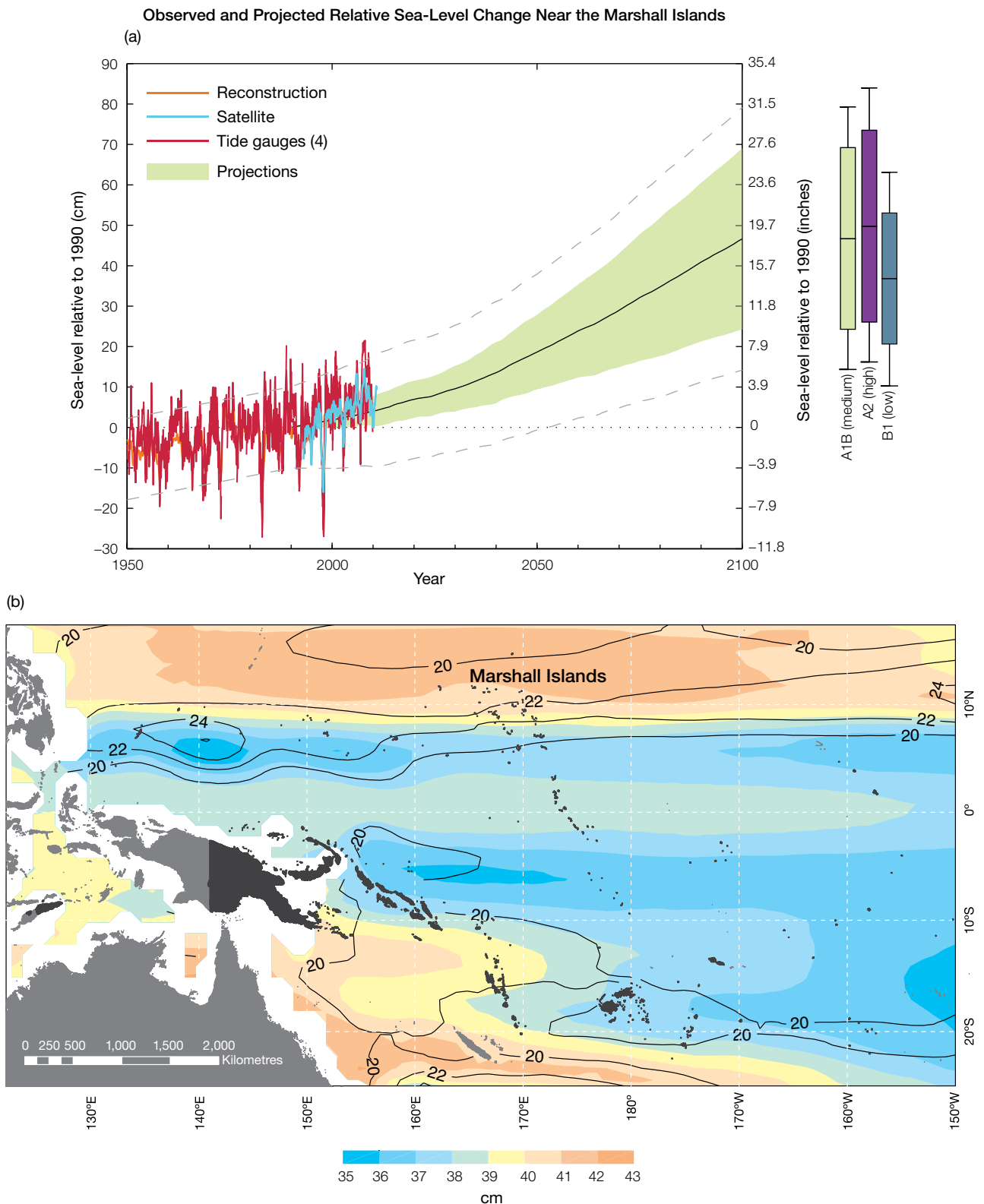
Figure 7.9: Observed and projected relative sea-level change near the Marshall Islands. (a) The observed in situ relative sea-level records are indicated in red, with the satellite record (since 1993) in light blue. The gridded sea level at the Marshall Islands (since 1950, from Church and White (in press)) is shown in orange. The projections for the A1B (medium) emissions scenario (5–95% uncertainty range) are shown by the green shaded region from 1990–2100. The range of projections for the B1 (low), A1B (medium) and A2 (high) emissions scenarios by 2100 are also shown by the bars on the right. The dashed lines are an estimate of interannual variability in sea level (5–95% range about the long-term trends) and indicate that individual monthly averages of sea level can be above or below longer-term averages. (b) The projections (in cm) for the A1B (medium) emissions scenario in the Marshall Islands region for the average over 2081–2100 relative to 1981–2000 are indicated by the shading, with the estimated uncertainty in the projections indicated by the contours (in cm).

7.7.6 Projections Summary

The projections presented in Section 7.7 are summarised in Table 7.4 (northern Marshall Islands) and Table 7.5 (southern Marshall Islands). For detailed information regarding the various uncertainties associated with the table values, refer to the preceding text in Sections 7.7 and 1.7, in addition to Chapters 5 and 6 in Volume 1. When interpreting the differences between projections for the B1 (low), A1B (medium) and A2 (high) emissions scenarios, it is also important to consider the emissions pathways associated with each scenario (Volume 1, Figure 4.1) and the fact that a slightly different subset of models was available for each (Volume 1, Appendix 1).

Table 7.4: Projected change in the annual and seasonal mean climate for the northern Marshall Islands, under the B1 (low; blue), A1B (medium; green) and A2 (high; purple) emissions scenarios. Projections are given for three 20-year periods centred on 2030 (2020–2039), 2055 (2046–2065) and 2090 (2080–2099), relative to 1990 (1980–1999). Values represent the multi-model mean change ± twice the inter-model standard deviation (representing approximately 95% of the range of model projections), except for sea level where the estimated mean change and the 5–95% range are given (as they are derived directly from the Intergovernmental Panel on Climate Change Fourth Assessment Report values). The confidence (Section 1.7.2) associated with the range and distribution of the projections is also given (indicated by the standard deviation and multi-model mean, respectively). See Volume 1, Appendix 1 for a complete listing of CMIP3 models used to derive these projections.

Variable	Season	2030	2055	2090	Confidence
Surface air temperature (°F)	Annual	+1.1 ± 0.7	+1.9 ± 0.9	+2.7 ± 1.3	High
		+1.4 ± 0.8	+2.7 ± 1.0	+4.2 ± 1.6	
		+1.3 ± 0.5	+2.5 ± 0.8	+5.0 ± 1.2	
Surface air temperature (°C)	Annual	+0.6 ± 0.4	+1.0 ± 0.5	+1.5 ± 0.7	High
		+0.8 ± 0.4	+1.5 ± 0.6	+2.3 ± 0.9	
		+0.7 ± 0.3	+1.4 ± 0.4	+2.8 ± 0.7	
Maximum temperature (°F)	1-in-20-year event	N/A	+1.8 ± 1.3	+2.3 ± 1.4	Low
			+2.5 ± 1.4	+4.0 ± 2.2	
			+2.5 ± 0.9	+4.9 ± 2.3	
Maximum temperature (°C)	1-in-20-year event	N/A	+1.0 ± 0.7	+1.3 ± 0.8	Low
			+1.4 ± 0.8	+2.2 ± 1.2	
			+1.4 ± 0.5	+2.7 ± 1.3	
Minimum temperature (°F)	1-in-20-year event	N/A	+2.2 ± 2.9	+3.1 ± 2.9	Low
			+2.7 ± 2.9	+4.1 ± 3.4	
			+2.5 ± 4.5	+4.9 ± 2.9	
Minimum temperature (°C)	1-in-20-year event	N/A	+1.2 ± 1.6	+1.7 ± 1.6	Low
			+1.5 ± 1.6	+2.3 ± 1.9	
			+1.4 ± 2.5	+2.7 ± 1.6	
Total rainfall (%)*	Annual	+3 ± 14	+2 ± 4	+3 ± 9	Moderate
		+1 ± 9	+5 ± 12	+11 ± 45	
		+3 ± 13	+7 ± 24	+12 ± 25	
Dry season rainfall (%)*	November-April	+2 ± 21	+4 ± 18	+2 ± 25	Moderate
		+4 ± 14	+9 ± 32	+16 ± 64	
		+5 ± 24	+13 ± 42	+20 ± 49	
Wet season rainfall (%)*	May-October	+3 ± 14	+2 ± 7	+3 ± 7	Moderate
		-1 ± 13	+4 ± 10	+9 ± 39	
		+3 ± 10	+6 ± 18	+9 ± 21	
Sea-surface temperature (°F)	Annual	+1.3 ± 0.9	+2.0 ± 1.3	+2.7 ± 1.6	Moderate
		+1.4 ± 1.1	+2.5 ± 1.3	+4.1 ± 1.8	
		+1.3 ± 0.7	+2.5 ± 1.1	+4.9 ± 1.3	
Sea-surface temperature (°C)	Annual	+0.7 ± 0.5	+1.1 ± 0.7	+1.5 ± 0.9	Moderate
		+0.8 ± 0.6	+1.4 ± 0.7	+2.3 ± 1.0	
		+0.7 ± 0.4	+1.4 ± 0.6	+2.7 ± 0.7	
Aragonite saturation state (Ωar)	Annual maximum	+3.4 ± 0.1	+3.2 ± 0.1	+3.0 ± 0.1	Moderate
		+3.3 ± 0.1	+3.0 ± 0.1	+2.6 ± 0.2	
		+3.4 ± 0.1	+3.0 ± 0.1	+2.4 ± 0.1	
Mean sea level (inches)	Annual	+3.5 (1.6–5.9)	+7.5 (3.9–10.6)	+13.0 (7.1–18.5)	Moderate
		+3.5 (1.6–5.9)	+8.3 (4.3–12.6)	+16.1 (8.3–23.6)	
		+3.9 (1.2–6.3)	+7.9 (4.3–11.8)	+16.5 (8.7–24.4)	
Mean sea level (cm)	Annual	+10 (4–15)	+19 (10–27)	+33 (18–47)	Moderate
		+10 (4–15)	+21 (11–32)	+41 (21–60)	
		+9 (3–16)	+20 (11–30)	+42 (22–62)	

*The MIROC3.2(hires) model was eliminated in calculating the rainfall projections, due to its inability to accurately simulate present-day activity of the Intertropical Convergence Zone (Volume 1, Section 5.5.1).

Table 7.5: Projected change in the annual and seasonal mean climate for the southern Marshall Islands, under the B1 (low; blue), A1B (medium; green) and A2 (high; purple) emissions scenarios. Projections are given for three 20-year periods centred on 2030 (2020–2039), 2055 (2046–2065) and 2090 (2080–2099), relative to 1990 (1980–1999). Values represent the multi-model mean change ± twice the inter-model standard deviation (representing approximately 95% of the range of model projections), except for sea level where the estimated mean change and the 5–95% range are given (as they are derived directly from the Intergovernmental Panel on Climate Change Fourth Assessment Report values). The confidence (Section 1.7.2) associated with the range and distribution of the projections is also given (indicated by the standard deviation and multi-model mean, respectively). See Volume 1, Appendix 1 for a complete listing of CMIP3 models used to derive these projections.

Variable	Season	2030	2055	2090	Confidence
Surface air temperature (°F)	Annual	+1.2 ± 0.8	+2.0 ± 1.0	+2.8 ± 1.4	Moderate
		+1.4 ± 0.9	+2.7 ± 1.2	+4.3 ± 1.7	
		+1.3 ± 0.5	+2.6 ± 0.8	+5.1 ± 1.2	
Surface air temperature (°C)	Annual	+0.7 ± 0.4	+1.1 ± 0.6	+1.6 ± 0.8	Moderate
		+0.8 ± 0.5	+1.5 ± 0.7	+2.4 ± 0.9	
		+0.7 ± 0.3	+1.4 ± 0.4	+2.8 ± 0.7	
Maximum temperature (°F)	1-in-20-year event	N/A	+1.8 ± 0.9	+2.3 ± 1.4	Low
			+2.5 ± 1.4	+4.0 ± 2.2	
			+2.5 ± 0.7	+4.9 ± 2.7	
Maximum temperature (°C)	1-in-20-year event	N/A	+1.0 ± 0.5	+1.3 ± 0.8	Low
			+1.4 ± 0.8	+2.2 ± 1.2	
			+1.4 ± 0.4	+2.7 ± 1.5	
Minimum temperature (°F)	1-in-20-year event	N/A	+2.3 ± 2.7	+3.2 ± 2.7	Low
			+2.7 ± 2.9	+4.1 ± 3.2	
			+2.7 ± 2.7	+4.9 ± 3.2	
Minimum temperature (°C)	1-in-20-year event	N/A	+1.3 ± 1.5	+1.8 ± 1.5	Low
			+1.5 ± 1.6	+2.3 ± 1.8	
			+1.5 ± 1.5	+2.7 ± 1.8	
Total rainfall (%)*	Annual	+2 ± 8	+5 ± 9	+7 ± 11	Moderate
		+2 ± 7	+5 ± 11	+10 ± 16	
		+3 ± 9	+6 ± 13	+10 ± 19	
Dry season rainfall (%)*	November-April	0 ± 13	+5 ± 12	+5 ± 14	Moderate
		+2 ± 13	+5 ± 21	+10 ± 25	
		+3 ± 14	+7 ± 19	+9 ± 27	
Wet season rainfall (%)*	May-October	+3 ± 10	+6 ± 11	+8 ± 13	Moderate
		+3 ± 9	+5 ± 9	+10 ± 17	
		+3 ± 10	+6 ± 14	+11 ± 23	
Sea-surface temperature (°F)	Annual	+0.6 ± 0.5	+1.1 ± 0.6	+1.5 ± 0.8	Moderate
		+0.7 ± 0.6	+1.4 ± 0.6	+2.2 ± 0.9	
		+0.7 ± 0.4	+1.3 ± 0.5	+2.6 ± 0.7	
Sea-surface temperature (°C)	Annual	+0.3 ± 0.3	+0.6 ± 0.3	+0.8 ± 0.4	Moderate
		+0.4 ± 0.3	+0.8 ± 0.3	+1.2 ± 0.5	
		+0.4 ± 0.2	+0.7 ± 0.3	+1.4 ± 0.4	
Aragonite saturation state (Ωar)	Annual maximum	+3.4 ± 0.2	+3.1 ± 0.1	+3.0 ± 0.2	Moderate
		+3.3 ± 0.1	+3.0 ± 0.2	+2.6 ± 0.2	
		+3.3 ± 0.2	+3.0 ± 0.1	+2.4 ± 0.2	
Mean sea level (inches)	Annual	+3.5 (1.6–5.9)	+7.5 (3.9–10.6)	+13.0 (7.1–18.5)	Moderate
		+3.5 (1.6–5.9)	+8.3 (4.3–12.6)	+16.1 (8.3–23.6)	
		+3.9 (1.2–6.3)	+7.9 (4.3–11.8)	+16.5 (8.7–24.4)	
Mean sea level (cm)	Annual	+10 (4–15)	+19 (10–27)	+33 (18–47)	Moderate
		+10 (4–15)	+21 (11–32)	+41 (21–60)	
		+9 (3–16)	+20 (11–30)	+42 (22–62)	

*The MIROC3.2(hires) model was eliminated in calculating the rainfall projections, due to its inability to accurately simulate present-day activity of the Intertropical Convergence Zone (Volume 1, Section 5.5.1).